

1 **Title: An environmental determinant of viral respiratory disease**

2 Authors:

3 Yeon-Woo Choi<sup>1,†</sup>, PhD

4 Alexandre Tuel<sup>1,†,\*</sup>, MSc

5 Elfatih A. B. Eltahir<sup>1</sup>, PhD

6

7 **ABSTRACT:**

8 The evident seasonality of influenza suggests a significant role for weather and climate as one of  
9 several determinants of viral respiratory disease (VRD), including social determinants which  
10 play a major role in shaping these phenomena. Based on the current mechanistic understanding  
11 of how VRDs are transmitted by small droplets, we identify an environmental variable, Air  
12 Drying Capacity (ADC), as an atmospheric state-variable with significant and direct relevance to  
13 the transmission of VRD. ADC dictates the evolution and fate of droplets under given  
14 temperature and humidity conditions. The definition of this variable is rooted in the Maxwell  
15 theory of droplet evolution via coupled heat and mass transfer between droplets and the  
16 surrounding environment. We present the climatology of ADC, and compare its observed  
17 distribution in space and time to the observed prevalence of influenza and COVID-19 from  
18 extensive global data sets. Globally, large ADC values appear to significantly constrain the  
19 observed transmission and spread of VRD, consistent with the significant coherency of the  
20 observed seasonal cycles of ADC and influenza. Our results introduce a new environmental  
21 determinant, rooted in the mechanism of VRD transmission, with potential implications for

1

22 explaining seasonality of influenza, and for describing how environmental conditions may  
23 impact to some degree the evolution of similar VRDs, such as COVID-19.

---

24 <sup>1</sup>Ralph M. Parsons Laboratory, Massachusetts Institute of Technology, Cambridge,  
25 Massachusetts 02139, USA

26 † equal contribution

27 \* e-mail: [atuel@mit.edu](mailto:atuel@mit.edu)

28 TEL: (617) 253-6596

## 29 **Main**

30 The spread of Viral Respiratory Diseases (VRDs), like influenza and COVID-19, is shaped by a  
31 combination of social, biological and environmental determinants. Social determinants include  
32 behavioural aspects (settlement density, mobility, personal hygiene, vaccination, social  
33 distancing, etc.) that affect the transmission of the disease. Biological determinants are defined  
34 here as characteristics of the pathogen itself including its response to abiotic factors, and the  
35 nature of the human immune response to it. Finally, environmental determinants are defined here  
36 as the set of environmental conditions that impact the intensity of the disease transmission  
37 process. (For example, how much a virus tolerates extreme temperature is a biological  
38 determinant, while how extreme temperature impacts the transmission of the virus is an  
39 environmental determinant.) Most public policy approaches to limit the spread of VRDs  
40 typically rely on manipulating social behaviours through emphasis on personal hygiene, social  
41 distancing and vaccination, and COVID-19 is no exception. Still, the dynamics and average  
42 prevalence of VRDs exhibit substantial variability across countries. Influenza is most widespread  
43 in the mid-latitudes,<sup>1</sup> and in the case of COVID-19, some countries have clearly experienced  
44 widespread transmission and an explosive growth in cases, while in others, the outbreak seems  
45 much more constrained.<sup>2-4</sup> It is evident that social determinants play a major role in controlling  
46 transmission, especially given the success of social distancing policies implemented in response  
47 to COVID-19. However, this does not necessarily imply that the environment plays no role in  
48 shaping VRD spread, as highlighted by the clear seasonality of influenza in mid-latitude  
49 countries.<sup>1</sup>

50 We still do not have a definite understanding of the biological determinants of VRDs. Laboratory  
51 experiments have suggested that ambient temperature and absolute humidity affected the  
52 survival of several VRD pathogens,<sup>5-7</sup> although the effect of temperature seems weak in the case  
53 of the SARS-CoV-2 virus responsible for COVID-19<sup>8</sup> (Fig. S1). High UV radiation is also  
54 believed to suppress viral activity and infectivity in the case of influenza viruses<sup>9</sup> and possibly  
55 SARS-CoV-2.<sup>10</sup> Additionally, evidence has emerged that viral shedding in mammals is enhanced  
56 at low temperatures,<sup>11</sup> making the case for strong biological controls on VRD prevalence.  
57 Yet, because VRDs are primarily transmitted by droplets exhaled by infected subjects,  
58 environmental conditions may also play a major role in shaping their spread.<sup>12,13</sup> Previous studies  
59 have argued that cold and dry environments were conducive to the survival and transport of  
60 VRD-infected droplets, unlike warm and humid environments.<sup>1,6</sup> This hypothesis seems  
61 supported by empirical relationships applied to country-level data,<sup>7,14,15,16</sup> though in the case of  
62 COVID-19 initial results suggest that weather and climate conditions may have limited effects  
63 on the spread of the disease.<sup>17,18</sup>  
64 One important limitation of such studies is their focus on temperature or humidity as separate  
65 covariates to understand or predict VRD prevalence. Different relationships are developed for  
66 tropical and mid-latitude countries<sup>1</sup> although the physics of droplets is the same. Additionally,  
67 relationships are sometimes found to be non-monotonic: in the case of COVID-19, the  
68 transmission efficiency may first be enhanced as temperature and absolute humidity drop, and  
69 then decline beyond a certain threshold.<sup>15</sup> Therefore, while evidence points to some degree of  
70 environmental control on VRD spread and prevalence, the lack of a consistent and physically-  
71 based framework makes it all the more difficult to assess.

72 Here, we propose a new atmospheric state-variable, named Air Drying Capacity (ADC), rooted  
73 in the current mechanistic understanding of how transmission takes place by small droplets.  
74 ADC is defined as the rate of decrease with time of a droplet surface area, given ambient  
75 temperature and humidity. As such, ADC integrates naturally the effects of both temperature and  
76 humidity based on their relative roles in dictating the decrease of the droplet surface area. ADC  
77 offers a consistent, physically-based framework to assess the effect of environmental conditions  
78 on global and seasonal patterns of VRD prevalence.

79

## 80 **Methods**

### 81 **Droplet Theory of VRD Transmission**

82 VRDs are believed to be transmitted by droplets exhaled by infected subjects.<sup>19-22</sup> The size of  
83 exhaled droplets by human typically ranges from about 0.5  $\mu\text{m}$  in breathing, and increases with  
84 speech up to about 10  $\mu\text{m}$ .<sup>23</sup> Larger droplets, up to 200-300  $\mu\text{m}$ , can be emitted by sneezing or  
85 coughing.<sup>24</sup> After emission, droplets can contaminate nearby surfaces, or disperse as aerosols and  
86 may infect subjects who inhale them. This idea, first developed by Wells,<sup>25</sup> led to the  
87 discrimination of “large” and “small” droplets, and has since then influenced strategies to control  
88 the spread of infection according to whether the disease was thought to be transmitted primarily  
89 through large or small droplets.<sup>26</sup> Droplet diameter cut-offs usually range between 5 and 10 $\mu\text{m}$ ,<sup>27</sup>  
90 and the typical associated distance varies between 1.5 and 2m.<sup>28</sup> More recent studies have  
91 shown, however, that these arbitrary droplet size cut-offs do not reflect the actual trajectories of  
92 exhaled droplets. The dynamics of droplet evaporation and evolution are indeed very dependent  
93 on the characteristics of the complex multiphase turbulent flow which the droplets exist in<sup>29</sup> as

94 well as background environmental conditions.<sup>12</sup> While influenza transmission has been shown to  
95 occur through both the large and small droplet route,<sup>21</sup> at this stage, COVID-19 is still believed  
96 to be mainly transmitted by the large droplet path,<sup>30</sup> although aerosol transmission may also be  
97 possible.<sup>31</sup> In any case, exhaled droplets are still the major infection route, which implies that  
98 environmental controls on droplet evaporation and disappearance may play an important role in  
99 determining the spread of the disease.

100

### 101 **A proposed environmental determinant: Atmospheric Drying Capacity (ADC)**

102 Droplet growth theory under given environmental conditions goes back to the pioneering work  
103 of Maxwell,<sup>32</sup> who first posited that steady-state dynamics of spherical droplets at rest in  
104 isotropic gaseous media were controlled by the equilibrium between heat and mass exchange at  
105 their surface. Both mass and heat transfer involve ambient temperature and humidity, and are  
106 therefore strongly constrained by environmental conditions. In steady-state, mass and heat  
107 transfer exactly compensate, and one finds that the radius  $r$  of a droplet evolves according to<sup>33</sup>:

$$108 \quad r \frac{dr}{dt} = \frac{(RH - 1)}{\left(\frac{L_v}{R_v T_a} - 1\right) \frac{L_v \rho}{K T_a} + \frac{\rho R_v T_a}{e_s(T_a) D}} \equiv f(T_a, RH) \quad (4)$$

109 where  $RH$  is the ambient relative humidity,  $T_a$  the ambient temperature,  $R_v$  the specific gas  
110 constant for water vapour,  $\rho$  liquid water density,  $L_v$  the latent heat of vaporisation,  $K$  the  
111 thermal conductivity of air,  $D$  the water vapour diffusion coefficient, and  $e_s(T)$  the saturation  
112 vapor pressure at temperature  $T$  given by the Clausius-Clapeyron equation. We then define the  
113 Air Drying Capacity (ADC, in mm<sup>2</sup>/hr) as the rate of decrease of the droplet surface area:

$$114 \quad ADC(T_a, RH) \equiv -3.6 \times 8\pi \times 10^9 \times f(T_a, RH) \quad (5)$$

115 ADC is therefore an atmospheric state-variable uniquely related to air temperature and humidity  
116 only. For typical ranges of air temperature and humidity, ADC varies between 0 and 15 mm<sup>2</sup>/hr  
117 (Fig. 1-a,b). It is a linear function of both relative and specific humidity, but a non-linear  
118 function of temperature, consistent with the Clausius-Clapeyron law. ADC strongly controls the  
119 time it takes for a free-falling droplet to evaporate, and therefore the diameter cut-off between  
120 “large” droplets, that reach the ground before evaporating, and “small” droplets, which turn into  
121 aerosols (Fig. 1-c). At low ADC values (0-1 mm<sup>2</sup>/hr), only droplets larger than about 25µm will  
122 be able to contaminate nearby surfaces, while for high ADC (>10 mm<sup>2</sup>/hr) that threshold moves  
123 up to 60µm. Additionally, the potential range of such large droplets is also severely reduced as  
124 ADC increases, because they can remain in the air for a significantly shorter time (Fig. 1-c, Fig.  
125 S2). Small (<10µm) droplets – a size typically emitted during normal speech – while never able  
126 to contaminate surfaces under the typical range of ADC values, can however potentially be  
127 inhaled by subjects in the vicinity of the emitter. Their fate is largely controlled by ADC: a 10µm  
128 droplet will evaporate in as much as 25s or as less as 0.5s depending on the background ADC.  
129 This may be particularly relevant for VRD pathogens whose infectivity declines once in the dry  
130 aerosol phase.

131

## 132 **Data**

133 6-hourly temperature, dew point temperature and surface pressure data at 0.75° spatial resolution  
134 between 1979 and 2018 were obtained from the ERA-Interim reanalysis<sup>34</sup> (available at  
135 <http://apps.ecmwf.int/datasets/>). Since ERA-Interim is only available up to 2019, we used 6-

136 hourly ERA5T<sup>35</sup> data ( $0.25^\circ \times 0.25^\circ$  horizontal resolution) for the recent February-April 2020  
137 period.  
138 Daily COVID-19 epidemiological data compiled by the Johns Hopkins University Center for  
139 Systems Science and Engineering is available at country-scale since 22 January 2020 at  
140 <https://data.humdata.org/>. The most up-to-date COVID data for each US state at a daily temporal  
141 resolution is taken from the COVID Tracking Project (<https://covidtracking.com/data/>).  
142 Population data for world countries and US states was downloaded from  
143 <https://www.worldometers.info/world-population> and <https://www.wikipedia.org>, respectively.  
144 Weekly laboratory confirmed influenza cases by country for the period October 15<sup>th</sup>, 1995 to  
145 August 31<sup>st</sup>, 2019 are retrieved from the World Health Organization’s FluNet database,  
146 accessible at [https://www.who.int/influenza/gisrs\\_laboratory/flunet/en/](https://www.who.int/influenza/gisrs_laboratory/flunet/en/). The dataset consists in  
147 weekly totals of identified influenza A and B cases, along with the number of subjects tested. It  
148 suffers from both a sampling bias (variations with time and space in the number of people  
149 tested), and a reporting bias (reports are not available consistently over time). We use two  
150 indices of influenza prevalence to separately address these biases. First, we define an “influenza  
151 frequency index”, defined weekly as the number of positive influenza A and B cases divided by  
152 the number of tested subjects. Second, we define a “normalized influenza prevalence (NIP)”  
153 index based on the approach of Deyle et al.<sup>14</sup> as the number of positive cases divided by  
154 population (linearly interpolated over time to account for population trends), and multiplied by  
155 the average number of annual reports for all countries divided by the average number of annual  
156 reports for the country in question:

$$157 \quad NIP(t, C) = \frac{\# \text{ positives, country } C, \text{ week } t}{\text{population, country } C} \times \frac{\text{avg \# weekly reports, all countries}}{\text{avg \# weekly reports, country } C}$$



158 (see supplementary methods for more details).

159

## 160 **Results**

### 161 **Climatology of ADC**

162 The spatial distribution of annual-average ADC shows a somewhat meridionally symmetric  
163 pattern. The lowest values, between 0-2 mm<sup>2</sup>/hr, can be found above 60° latitude in each  
164 hemisphere and over land areas around the equator (Fig. 2-a). The subtropics in each hemisphere  
165 exhibit high ADC values, particularly over the large deserts of North Africa and southwest Asia  
166 where temperature is high and humidity is low. Australia, India and the Western United States  
167 are all characterised by relatively high ADCs. The situation during winter and spring is overall  
168 quite similar, though with notable regional differences (Fig. 2-b,e). Europe and Eastern North  
169 America both show particularly low ADC values during winter, much lower than in China where  
170 ADC remains mostly above 2 mm<sup>2</sup>/hr. ADC over south-eastern Brazil is also at its minimum  
171 (Fig. 2-e). By contrast, most of Africa, and specifically its large population centres of Ethiopia,  
172 Egypt and Nigeria, all show high ADCs. The same can be said for India, particularly during  
173 spring. However, consistent with the summer monsoon cycle, ADC becomes much higher during  
174 and after the monsoon season over Western Africa and the Sahel region, as well as India, as  
175 high-ADC bands move northwards with the rains (Fig. 2-c,d). Over Western Europe and Eastern  
176 North America, ADC increases during summer, but remains rather low at around 5 mm<sup>2</sup>/hr. A  
177 video showing the space-time evolution of ADC is included with Supplementary Information.

178

### 179 **Testing the relevance of ADC for VRD prevalence**

180 The spatial and temporal distribution of influenza cases is highly consistent with that of ADC  
181 (Figs. 3-a, 4-a,b). ADC appears to set a strong upper bound on influenza prevalence that applies  
182 to all countries with available data: influenza has very limited prevalence at ADCs of  $5 \text{ mm}^2/\text{hr}$   
183 or larger, and clearly increases as ADC approaches 0 (Figs. 3-a, 4-a,b). The annual cycles of  
184 ADC and influenza are also highly consistent, with a clear peak in the disease around when ADC  
185 is at its lowest (Fig. 3-c). Africa stands out due to high ADC values and low influenza  
186 prevalence, whereas Europe and North America have low ADCs and generally higher numbers  
187 of influenza cases (Fig. 4-a,b). While socio-economic factors also play a role in modulating the  
188 spread of the disease, it is striking that ADC still constrains the upper end of the range of  
189 observed prevalence, consistent with its effect on droplets – the vectors of transmission,  
190 particularly the rapid increase in the time needed for droplet evaporation as ADC approaches 0  
191 (Fig. S2). By contrast, air temperature (Fig. 3-b) and specific humidity (Fig. S3-a,c) do not show  
192 such clear relationships to influenza, although the annual cycle of temperature appears quite  
193 consistent with that of influenza prevalence (Fig. 3-d). Results for relative humidity do show  
194 some enhancement of influenza as the air becomes moister (Fig. S3-b), but its annual cycle  
195 seems quite off when compared to that of influenza incidence (Fig. S3-d).

196 Interestingly, the spatial distribution of ADC during winter and spring also shows some  
197 resemblance to the global map of confirmed COVID-19 cases (Fig. 4-c,d, Fig. S4). The disease  
198 hotspots of Europe and Eastern North America ( $>1000$  cases per million) both have extremely  
199 low ADCs, whereas China and the Western United States have fewer cases per million and larger  
200 ADC, despite also being highly connected to the rest of the world. COVID-19 prevalence in  
201 South America and Australia is lower (10-500 per million), and even less than that in Africa and

202 India. Naturally, many other factors come into play here, like connectivity to the rest of the  
203 world, population density and localisation within countries, and public policy measures like  
204 social distancing or lockdowns. The number of reported cases also suffers from biases, especially  
205 undercounting. Still, countries with low (respectively high) ADCs generally seem to correspond  
206 to higher (respectively lower) disease prevalence, a tendency that seems robust to considerations  
207 of income levels or test numbers performed by different countries (Fig. S5).

208

## 209 **Discussion and Conclusions**

210 VRDs are primarily transmitted between humans through droplets exhaled by infected hosts.  
211 Environmental determinants that affect the fate of these droplets can therefore influence  
212 transmission of these diseases. We introduced here a new variable, ADC, motivated by droplet  
213 growth theory first developed by Maxwell<sup>32</sup>. ADC includes the effects of both temperature and  
214 humidity on droplet evolution in the atmosphere. Compared to temperature, ADC turns out to set  
215 a much more coherent constraint on influenza prevalence (Fig. 3). The empirical relationship of  
216 ADC with the average prevalence of both influenza and COVID-19 for various world regions is  
217 consistent with its physical effects on the decay of droplets through which VRDs are transmitted.  
218 ADC directly constrains the evaporation of airborne droplets, potentially setting a strong upper  
219 bound on VRD spread and prevalence that appears valid regardless of socio-economic factor  
220 (Figs. 4, S5). It is important to note that ADC also indirectly impacts the survival of liquid  
221 droplets even once they have landed on surfaces; high-ADC conditions lead to rapid evaporation  
222 from a surface. The transmission of the viruses responsible for COVID-19 and influenza is thus  
223 likely impacted by ADC.

224 Significant relationships between temperature or humidity and influenza dynamics have been  
225 suggested in previous studies for individual countries<sup>14</sup> and temperate regions<sup>6</sup>, but it appears  
226 that neither variable, unlike ADC, is able to explain the observed global pattern of influenza  
227 prevalence (Figs. 3, S3). In particular, while specific humidity seems to have a strong effect on  
228 influenza virus survival, potentially affecting its transmission during the relatively low-specific  
229 humidity peak season in mid-latitude countries<sup>6</sup>, peak influenza in different countries occurs at  
230 both times of minimum and of maximum specific humidity<sup>1</sup>. The environmental determinant of  
231 VRD proposed in this study has important implications for consistently explaining the  
232 seasonality of influenza across the globe. Two kinds of favourable environments have been  
233 suggested for influenza transmission: “cold-dry” (as in mid-latitude countries) and “humid-  
234 rainy” (as in tropical countries),<sup>1</sup> in order to reconcile discrepancies in explaining seasonality of  
235 influenza at the global scale.<sup>36</sup> However, if specific humidity were the determinant variable  
236 impacting transmission, humid countries would hardly experience any influenza outbreaks,  
237 especially during their wet season. Two clusters of high influenza prevalence can be found in the  
238 WHO dataset, at both very low and very high humidity (Fig. S6). What they have in common are  
239 low ADC values, and in fact each cluster corresponds to the period of annual minimum ADC in  
240 mid-latitude and in tropical countries. The two proposed influenza regimes may therefore be  
241 reconciled by considering ADC framework proposed in this paper. While humidity and  
242 temperature may mimic influenza dynamics at the scale of individual countries,<sup>6,14</sup> these same  
243 relationships seem less valid when assumed for the world as whole and do not explain the large  
244 discrepancies in influenza prevalence between countries. At the global scale, it appears that the

245 environment's direct effect on droplets, the VRD transmission vectors, and described here using  
246 ADC, dominates over its biological effect on virus survival.

247 While ADC may only set an upper limit to VRD prevalence, social determinants like individual  
248 behaviour, socioeconomic conditions, healthcare expenditure, population density, cultural norms,  
249 etc. play a major role in shaping such diseases, and likely explain much of the spread in VRD  
250 prevalence below the ADC-dependent threshold. Strictly speaking, ADC describes the  
251 environmental conditions under which VRDs are likely to be transmitted. Whether or not  
252 transmission actually occurs depends, in addition to ADC, on several complex biological as well  
253 as social factors. As demonstrated in Figs. 3 and 4, the same value of ADC corresponds to a  
254 range of values of observed cases of VRD. That variability in spread is undoubtedly linked to the  
255 social and biologic factors independent of ADC, as well as the history of the disease in that  
256 location including seeding from other locations. However, the upper limit on the observed range  
257 of prevalence decreases over several orders of magnitude as ADC increases, highlighting the  
258 potentially important role of this variable.

259 Variations in ADC are consistent with the explosiveness of the COVID-19 outbreak in Europe  
260 and north-eastern America, where ADC is low, whereas regions with higher ADC have  
261 experienced a much slower growth in cases. In particular, Africa and India stand out by high  
262 ADC values and low COVID-19 prevalence (Fig. 4-a, Fig. 5). A recent study argued for a  
263 reduced transmission rate in Africa potentially linked to the environment, consistent with its  
264 higher ADC.<sup>4</sup> Admittedly, COVID-19 data is quite limited, and very much impacted by policy  
265 measures taken to limit disease spread. In addition, testing has been inconsistent across the  
266 world; in many countries, reported cases largely refer to individuals showing visible symptoms

267 of the disease, leaving out many asymptomatic cases. Similarly, influenza data is not free from  
268 biases (see Methods). This should make us careful in drawing final conclusions. Still, average  
269 influenza and COVID-19 prevalence show a similar and consistent relationship to ADC (Fig. 3).  
270 Since the high seasonality of influenza is coherent with that of ADC (Figs. 3-c), this suggests  
271 that COVID-19 may also follow ADC seasonality, with potential implications for the current  
272 disease hotspots of Europe and north-eastern America, where ADC will increase as summer  
273 approaches (Fig. 5). In regions of Asia outside India, where the seasonality of ADC is very  
274 limited, environmental determinants will probably not play much of a role in shaping COVID-19  
275 dynamics in the months to come. However, the situation may be more worrying in India and  
276 Western Africa, two regions where the summer monsoonal systems will bring low ADC  
277 conditions offering favourable conditions for the spread of the disease if effective preventive  
278 measures are not taken.

279 Nevertheless, our results present some important caveats. First, indoor heating and cooling will  
280 substantially move ADC away from its outdoor value, which we considered in our analysis.  
281 Transmission can occur indoors where temperature can be very different from outdoor  
282 conditions. Typically, in mid-latitudes, wintertime ADC is much higher inside than outside, and  
283 vice-versa during summer. Still, in regions where air conditioning and heating are available,  
284 conditions indoors should tend to exhibit much less seasonality than outdoors. In addition, the  
285 evident seasonality of influenza makes a strong case for the role of outdoor conditions, given that  
286 people spend much of their time indoors year-round<sup>36</sup>. The seasonality of VRDs may therefore  
287 primarily reflect outdoor ADC.

288 Second, biological determinants of virus survival may be strongly correlated to ADC, meaning  
289 that part of the ADC-VRD prevalence relationship may be explained by the effect of  
290 environmental conditions on the virus itself, and not on the transmission pathway. In particular,  
291 temperature is thought to affect the survival of influenza viruses<sup>5</sup>, though we fail to find a  
292 coherent signal in global data (Fig. 3-b). Similarly, in the case of influenza and, possibly,  
293 COVID-19, UV radiation is believed to be severely detrimental to viruses.<sup>9</sup> Low ADC is  
294 unmistakably associated with low incoming UV, but at higher levels the relationship becomes  
295 less clear (Fig. S7). Therefore, ADC and UV radiation may well interact and strengthen their  
296 respective effects.

297 As the COVID-19 pandemic progresses, better data will become available, and it will become  
298 possible to test for the robustness of the relationship between its prevalence and ADC values. So  
299 far, evidence points to an influenza-like behaviour, with a pronounced seasonality and mid-  
300 latitude countries most at risk from late fall to early spring. For the latter, environmental  
301 conditions will therefore probably be conducive to a second wave in late 2020, while in Western  
302 Africa and India, summer 2020 may bring about favourable conditions for efficient spread of the  
303 disease. However, as stressed earlier, conducive environmental conditions are not sufficient to  
304 cause VRD spread, and significant outbreaks triggered by social behaviour can occur even under  
305 relatively unfavourable environmental conditions.

## 306   **References**

- 307       1. Tamerius JD, Shaman J, Alonso WJ, et al. Environmental Predictors of Seasonal  
308       Influenza Epidemics across Temperate and Tropical Climates. *PLoS Pathog* 2013; **9**:  
309       e1003194.
- 310       2. Araujo MB, Naimi B. Spread of SARS-CoV-2 Coronavirus likely to be constrained by  
311       climate. *medRxiv* 2020; published online Apr 7. DOI:10.1101/2020.03.12.20034728  
312       (preprint).
- 313       3. Bukhari Q, Jameel Y. Will Coronavirus Pandemic Diminish by Summer? *SSRN* 2020;  
314       published online Mar 17. DOI:10.2139/ssrn.3556998 (preprint).
- 315       4. Cabore JW, Karamagi H, Kipruto H, et al. The potential effects of widespread  
316       community transmission of SARS-CoV-2 infection in the WHO African Region: a  
317       predictive model. *BMJ global health* 2020; accepted ([https://gh.bmj.com/pages/wp-](https://gh.bmj.com/pages/wp-content/uploads/sites/58/2020/05/BMJGH-The_potential_effects_of_widespread_community_transmission_of_SARS-CoV-2_infection_in_the_WHO_African_Region_a_predictive_model-Copy.pdf)  
318       content/uploads/sites/58/2020/05/BMJGH-  
319       The\_potential\_effects\_of\_widespread\_community\_transmission\_of\_SARS-CoV-  
320       2\_infection\_in\_the\_WHO\_African\_Region\_a\_predictive\_model-Copy.pdf).
- 321       5. Polozov IV., Bezrukov L, Gawrisch K, Zimmerberg J. Progressive ordering with  
322       decreasing temperature of the phospholipids of influenza virus. *Nat Chem Biol* 2008; **4**:  
323       248-255.
- 324       6. Shaman J, Kohn M. Absolute humidity modulates influenza survival, transmission, and  
325       seasonality. *Proc Natl Acad Sci USA* 2009; **106**: 3243–3248.



- 326 7. Wang J, Tang K, Feng K, Lv W. High Temperature and High Humidity Reduce the  
327 Transmission of COVID-19. *SSRN* 2020; published online Mar 10.  
328 DOI:10.2139/ssrn.3551767 (preprint).
- 329 8. Chin AWH, Chu JTS, Perera MRA, et al. Stability of SARS-CoV-2 in different  
330 environmental conditions. *medRxiv* 2020; published online Mar 27.  
331 DOI:10.1101/2020.03.15.20036673 (preprint).
- 332 9. Sagripanti JL, Lytle CD. Inactivation of influenza virus by solar radiation. *Photochem*  
333 *Photobiol* 2007; **83**: 1278–1282.
- 334 10. Homeland Security Science and Technology. Response to SARS-CoV-2 / COVID-19.  
335 Apr 20, 2020. [https://www.dhs.gov/sites/default/files/publications/panthr\\_covid-](https://www.dhs.gov/sites/default/files/publications/panthr_covid-19_fact_sheet_v13_27apr-final_0.pdf)  
336 [19\\_fact\\_sheet\\_v13\\_27apr-final\\_0.pdf](https://www.dhs.gov/sites/default/files/publications/panthr_covid-19_fact_sheet_v13_27apr-final_0.pdf) (accessed May 17, 2020).
- 337 11. Lowen AC, Mubareka S, Steel J, Palese P. Influenza virus transmission is dependent on  
338 relative humidity and temperature. *PLoS Pathog* 2007; **3**: 1470–1476.
- 339 12. Xie X, Li Y, Chwang ATY, Ho PL, Seto WH. How far droplets can move in indoor  
340 environments - revisiting the Wells evaporation-falling curve. *Indoor Air* 2007; **17**: 211–  
341 25.
- 342 13. Ishmatov A. Influence of weather and seasonal variations in temperature and humidity on  
343 supersaturation and enhanced deposition of submicron aerosols in the human respiratory  
344 tract. *Atmos Environ* 2020; **17**: 211–25.
- 345 14. Deyle ER, Maher MC, Hernandez RD, Basu S, Sugihara G. Global environmental drivers  
346 of influenza. *Proc Natl Acad Sci USA* 2016; **113**: 13081–13086.

- 347 15. Ficaretola GF, Rubolini D. Climate affects global patterns of COVID-19 early outbreak  
348 dynamics. *medRxiv* 2020; published online Apr 20. DOI:10.1101/2020.03.23.20040501  
349 (preprint).
- 350 16. Sajadi MM, Habibzadeh P, Vintzileos A, Shokouhi S, Miralles-Wilhelm F, Amoroso A.  
351 Temperature, humidity, and latitude analysis to predict potential spread and seasonality  
352 for COVID-19. *SSRN* 2020; published online Apr 6. DOI:10.2139/ssrn.3550308  
353 (preprint).
- 354 17. Luo W, Majumder MS, Liu D, et al. The role of absolute humidity on transmission rates  
355 of the COVID-19 outbreak. *medRxiv* 2020; published online Feb 17.  
356 DOI:10.1101/2020.02.12.20022467 (preprint).
- 357 18. Poirier C, Luo W, Majumder M, et al. The Role of Environmental Factors on  
358 Transmission Rates of the COVID-19 Outbreak: An Initial Assessment in Two Spatial  
359 Scales. *SSRN* 2020; published online Apr 16. DOI:10.2139/ssrn.3552677 (preprint).
- 360 19. Atkinson MP, Wein LM. Quantifying the routes of transmission for pandemic influenza.  
361 *Bull Math Biol* 2008; **70**: 820-867.
- 362 20. Stilianakis NI, Drossinos Y. Dynamics of infectious disease transmission by inhalable  
363 respiratory droplets. *J R Soc Interface* 2010; 1355-1366.
- 364 21. Cowling BJ, Ip DKM, Fang VJ, et al. Aerosol transmission is an important mode of  
365 influenza A virus spread. *Nat Commun* 2013; **4**: 1935.
- 366 22. Smieszek T, Lazzari G, Salathé M. Assessing the Dynamics and Control of Droplet- and  
367 Aerosol-Transmitted Influenza Using an Indoor Positioning System. *Sci Rep* 2019; **9**:  
368 2185.

- 369 23. Asadi S, Wexler AS, Cappa CD, Barreda S, Bouvier NM, Ristenpart WD. Aerosol  
370 emission and superemission during human speech increase with voice loudness. *Sci Rep*  
371 2019; **9**: 2348.
- 372 24. Han ZY, Weng WG, Huang QY. Characterizations of particle size distribution of the  
373 droplets exhaled by sneeze. *J R Soc Interface* 2013; **10**: 20130560.
- 374 25. Wells WF. On air-borne infection: Study II. Droplets and droplet nuclei. *Am J Epidemiol*  
375 1934; **20**: 611-618.
- 376 26. Bourouiba L. Turbulent Gas Clouds and Respiratory Pathogen Emissions: Potential  
377 Implications for Reducing Transmission of COVID-19. *JAMA - J Am Med Assoc* 2020;  
378 **323**: 1837-1838.
- 379 27. WHO. Infection prevention and control of epidemic- and pandemic-prone acute  
380 respiratory infections in health care. Apr, 2014.  
381 [https://www.who.int/csr/bioriskreduction/infection\\_control/publication/en/](https://www.who.int/csr/bioriskreduction/infection_control/publication/en/) (accessed  
382 May 17, 2020).
- 383 28. Siegel JD, Rhinehart E, Jackson M, Chiarello L. Guideline for isolation precautions:  
384 Preventing transmission of infectious agents in healthcare settings. 2007.  
385 <https://www.cdc.gov/infectioncontrol/guidelines/isolation/index.html> (accessed May 17.  
386 2020)
- 387 29. Bourouiba L, Dehandschoewercker E, Bush JWM. Violent respiratory events: On  
388 coughing and sneezing. *J Fluid Mech* 2014; **745**: 537-563.

- 389 30. WHO. Report of the WHO–China Joint Mission on Coronavirus Disease 2019 (COVID-  
390 19), 16–24 Feb, 2020. [https://www.who.int/docs/default-source/coronaviruse/who-china-](https://www.who.int/docs/default-source/coronaviruse/who-china-joint-mission-on-covid-19-final-report.pdf)  
391 [joint-mission-on-covid-19-final-report.pdf](https://www.who.int/docs/default-source/coronaviruse/who-china-joint-mission-on-covid-19-final-report.pdf) (accessed May 17, 2020).
- 392 31. Liu Y, Ning Z, Chen Y, et al. Aerodynamic analysis of SARS-CoV-2 in two Wuhan  
393 hospitals. *Nature* 2020; published online Apr 27. DOI: 10.1038/s41586-020-2271-3  
394 (preprint).
- 395 32. Maxwell JC. *The Scientific Papers of James Clerk Maxwell Vol. 1* (Dover, New York,  
396 2003)
- 397 33. Rogers RR, Yau MK. *A Short Course in Cloud Physics* (Pergamon, 1989).
- 398 34. Dee DP, Uppala SM, Simmons AJ, et al. The ERA-Interim reanalysis: Configuration and  
399 performance of the data assimilation system. *Q J R Meteorol Soc* 2011; **137**: 553-597.
- 400 35. Hersbach H, De Rosnay P, Bell B, et al. Operational global reanalysis: progress, future  
401 directions and synergies with NWP including updates on the ERA5 production status.  
402 *ERA Rep Ser* 2018. [https://www.ecmwf.int/en/elibrary/18765-operational-global-](https://www.ecmwf.int/en/elibrary/18765-operational-global-reanalysis-progress-future-directions-and-synergies-nwp)  
403 [reanalysis-progress-future-directions-and-synergies-nwp](https://www.ecmwf.int/en/elibrary/18765-operational-global-reanalysis-progress-future-directions-and-synergies-nwp) (accessed May 17, 2020).
- 404 36. Tamerius J, Nelson MI, Zhou SZ, Viboud C, Miller MA, Alonso WJ. Global influenza  
405 seasonality: Reconciling patterns across temperate and tropical regions. *Environ Health*  
406 *Perspect* 2011; **119**: 439-445.
- 407 37. Effros, R. M. et al. Dilution of respiratory solutes in exhaled condensates. *Am. J. Respir.*  
408 *Crit. Care Med.* 2002 **165**: 663–669.

409 **Author Contributions**

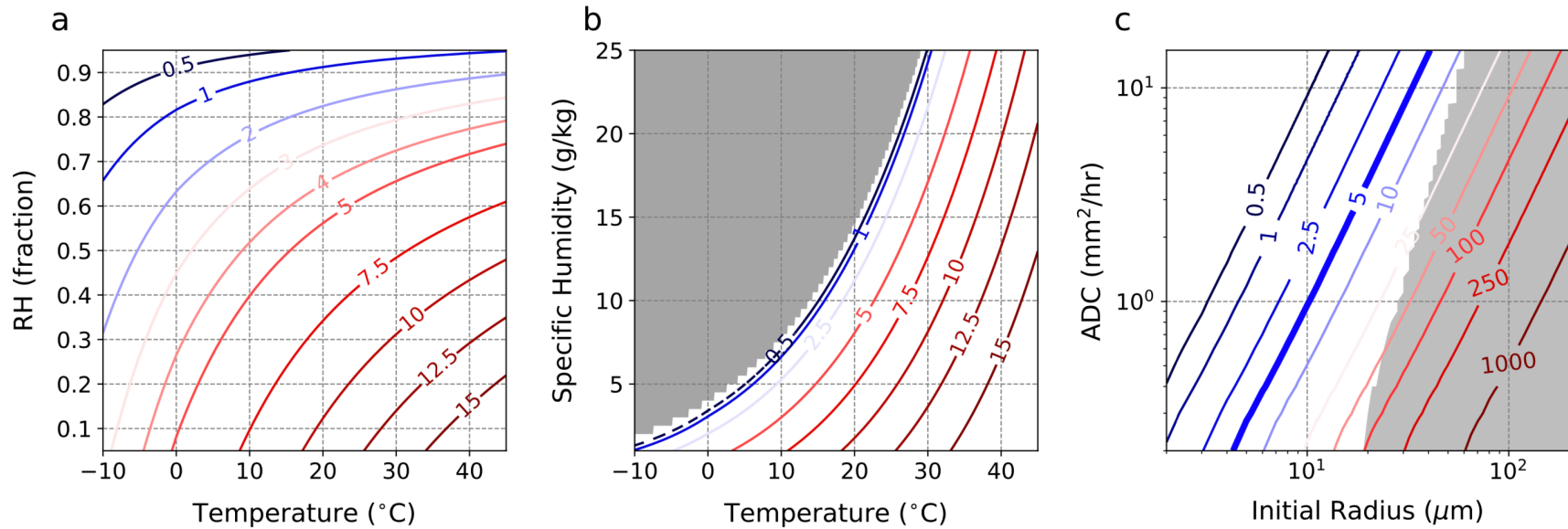
410 E. A. B. E. devised and supervised the study. Y. C. and A. T. carried out analyses. All authors  
411 contributed to the manuscript.

412 **Competing Interests**

413 The authors declare that they have no competing financial interests.

414 **Correspondence**

415 Correspondence and requests for materials should be addressed to [atuel@mit.edu](mailto:atuel@mit.edu).



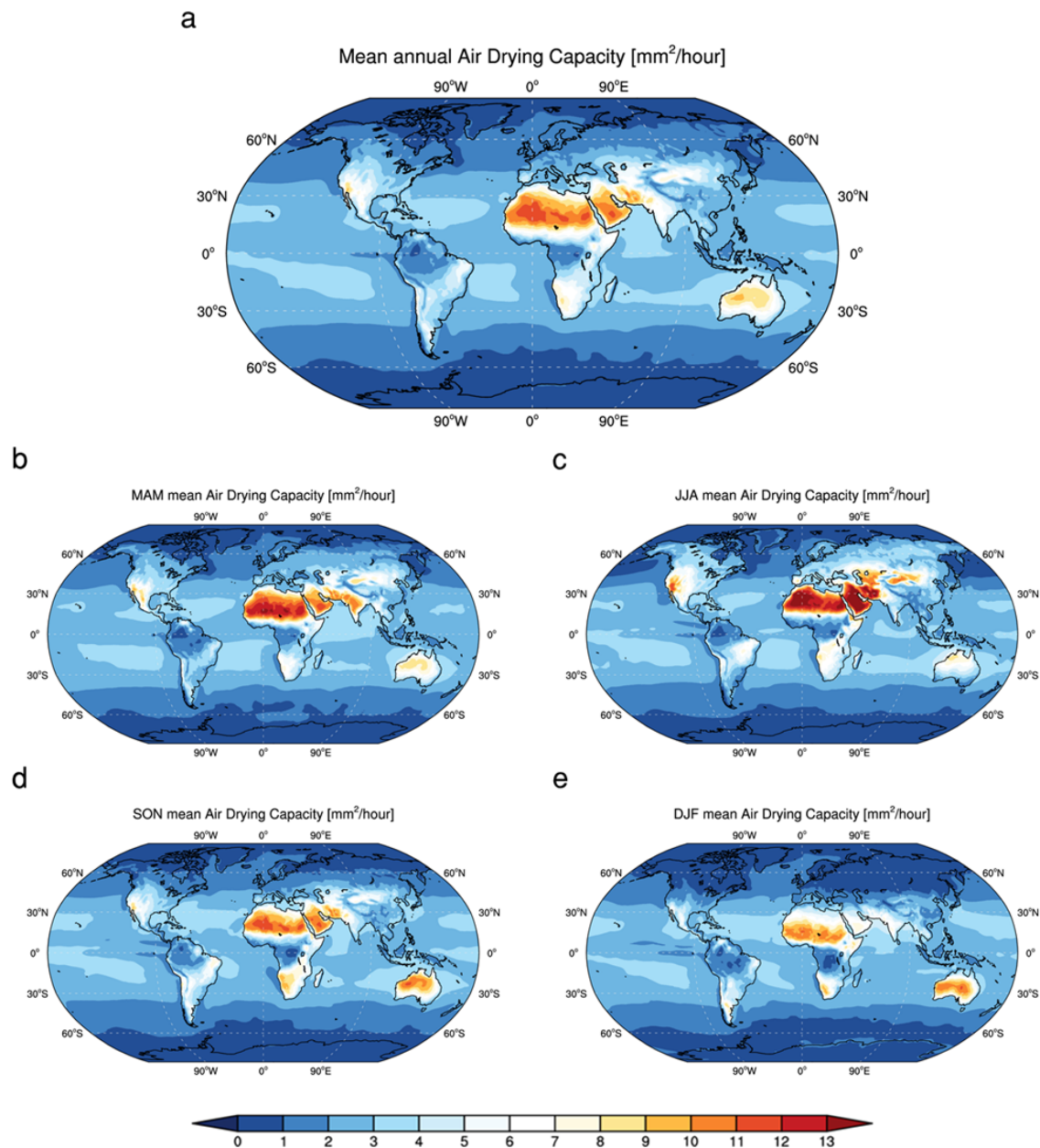
416

417 Figure 1. **ADC and environmental conditions.** (a-b) Air Drying Capacity (ADC, unit: mm<sup>2</sup>/hour) as a function of temperature and

418 (a) relative humidity and (b) specific humidity. The grey area in (b) indicates super-saturation. (c) Time to evaporation of free-falling,

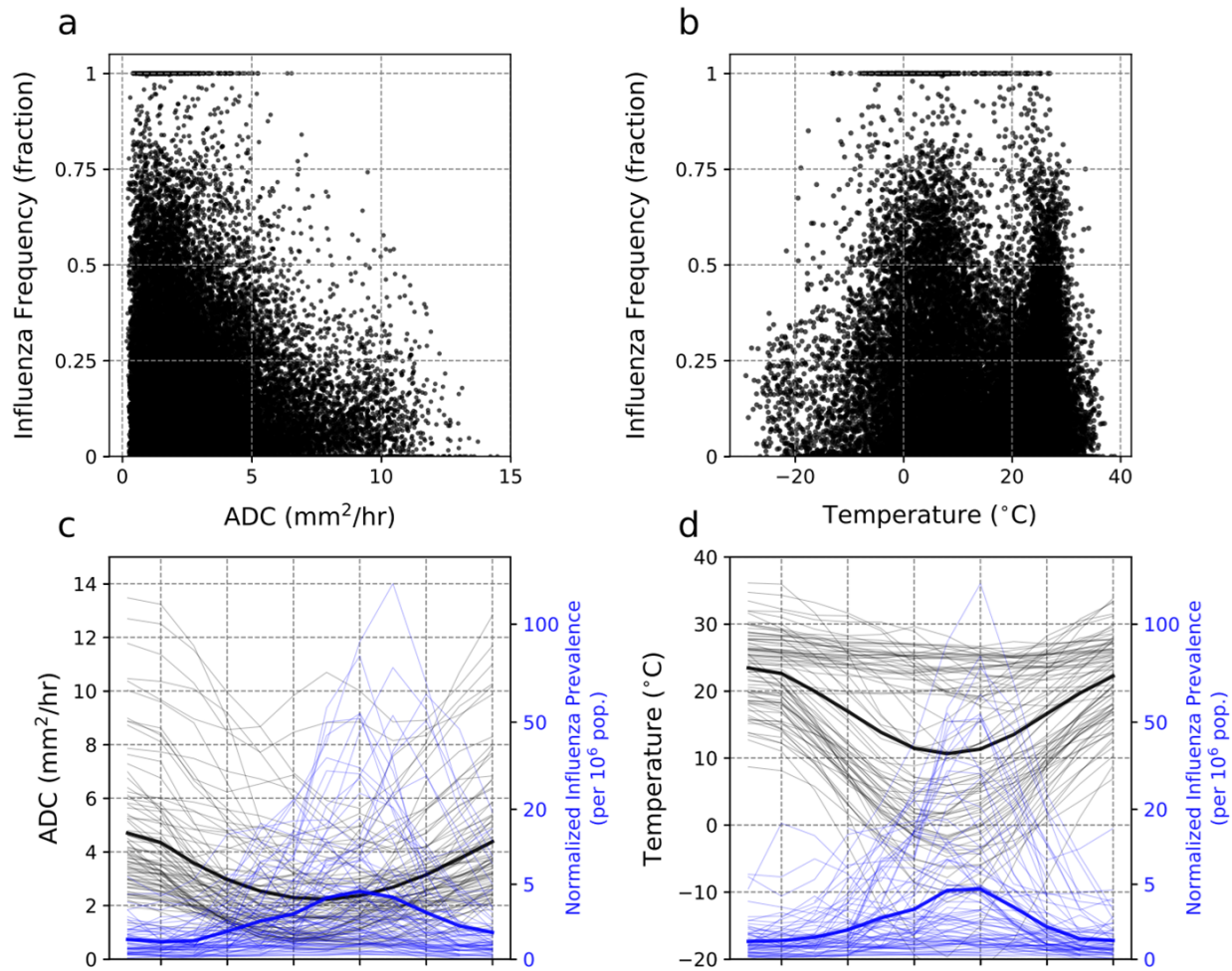
419 spherical water droplets as a function of ADC and initial droplet radius. The shaded area indicate the region where droplets reach the

420 ground before evaporating.



421

422 Figure 2. **Global distribution of ADC.** (a-e) Global map of (a) annual, (b) spring (March to  
423 May), (c) summer (June to August), (d) autumn (September to November), and (e) winter  
424 (December to February) average ADC for the period 1979-2018, calculated from the ERA-  
425 Interim dataset.



426

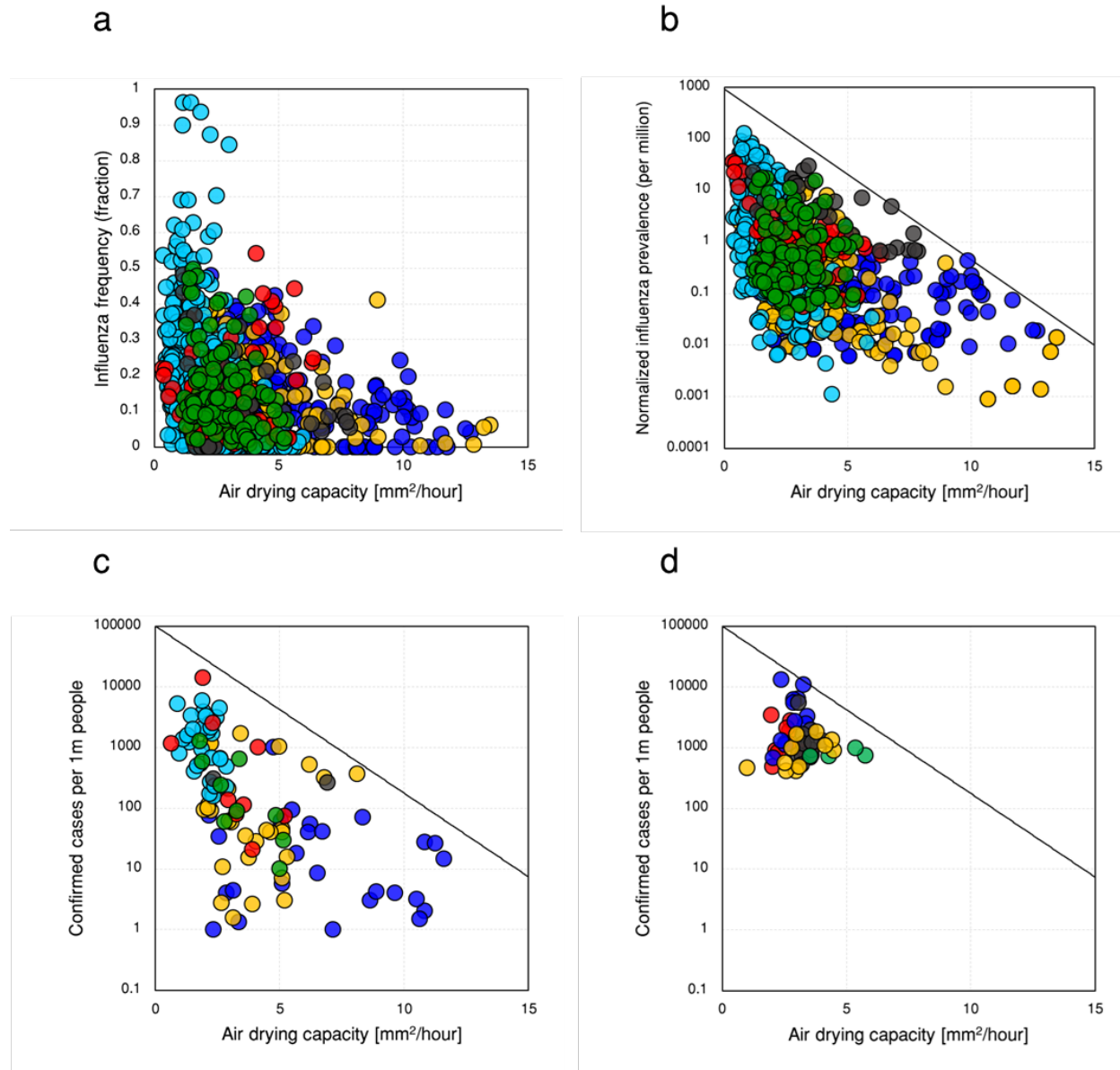
427 **Figure 3. Seasonal variation of ADC and prevalence of VRD.** (a-b) Weekly influenza

428 frequency against (a) ADC and (b) temperature. (c-d) Seasonal variation of normalised influenza

429 prevalence alongside (c) ADC and (d) temperature. In (c-d), the first month is defined for each of

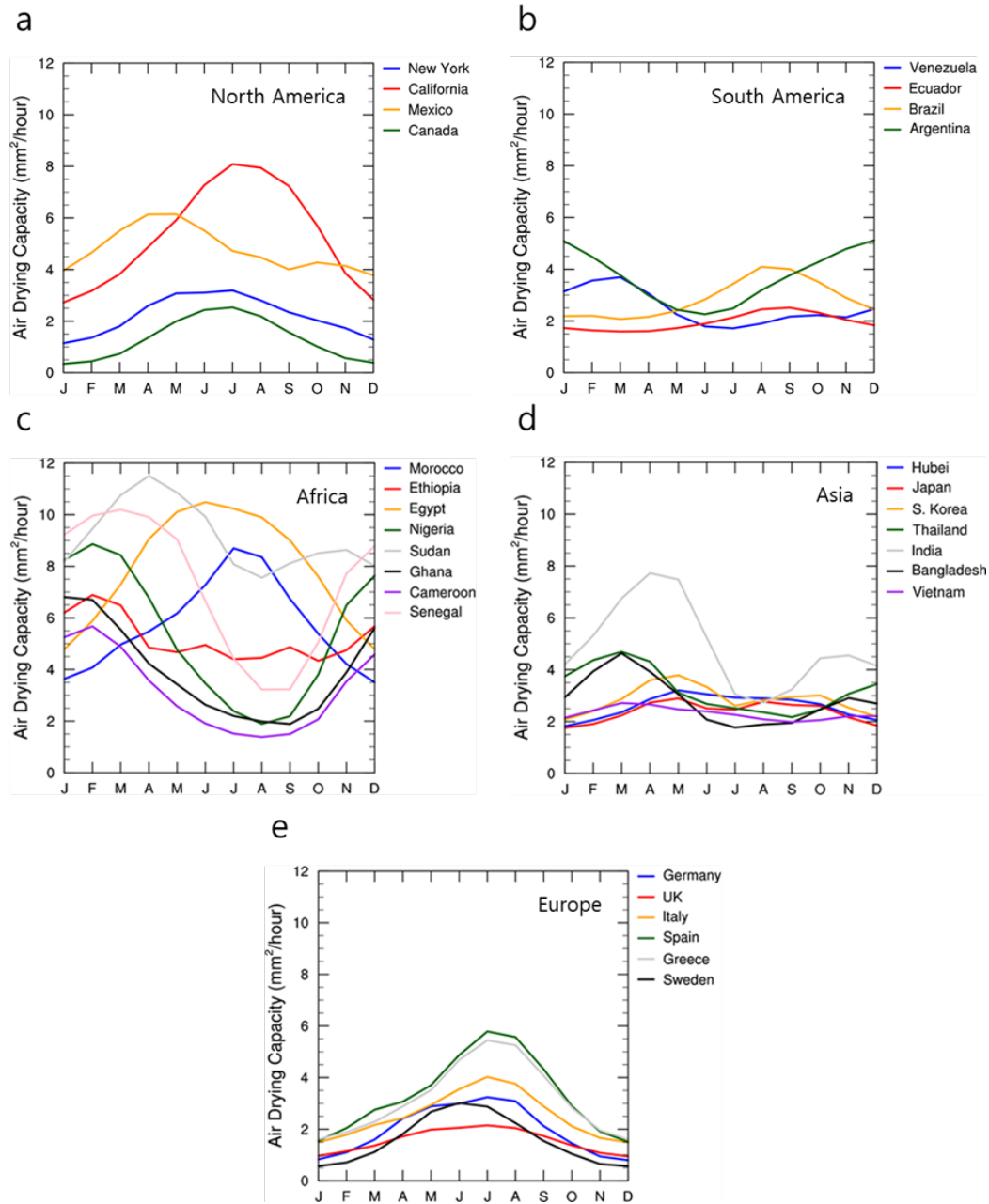
430 the 85 countries as the month with maximum ADC (c) or temperature (d).



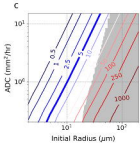
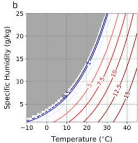
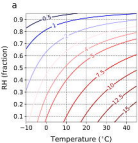


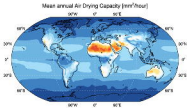
431  
432 **Figure 4. ADC and viral respiratory disease (VRD) prevalence.** (a-b) Long-term monthly-  
433 mean ADC against long-term monthly-mean (a) influenza A and B frequency, and (b)  
434 normalized influenza prevalence for 85 countries (Table S1) for the 1995-2019 period. (c)  
435 February-April 2020 ADC against concurrent accumulated confirmed COVID-19 cases for 108  
436 countries (Table S1). (d) Same as (c), but for the 50 US states. Red, green, light blue, yellow,  
437 blue and black colors in (a,b,c) respectively indicate North America, South America, Europe,  
25

438 Asia, Africa, and Oceania countries, and in (d) the Western, North-eastern, Midwestern, South-  
439 eastern, and South-western US states are represented by yellow, blue, red, black, and green  
440 colours, respectively.

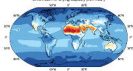


441  
442 Figure 5. **Seasonal variations of ADC.** (a-e) Monthly seasonal cycle of ADC for (a) North  
443 America, (b) South America, (c) Africa, (d) Asia, and (e) Europe. Data from 6-hourly ERA-  
444 Interim reanalysis.

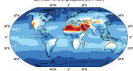


**a****b**

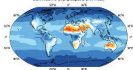
3000 mean Air Drying Capacity ( $\text{mm}^2/\text{hour}$ )

**c**

1800 mean Air Drying Capacity ( $\text{mm}^2/\text{hour}$ )

**d**

9000 mean Air Drying Capacity ( $\text{mm}^2/\text{hour}$ )

**e**

9000 mean Air Drying Capacity ( $\text{mm}^2/\text{hour}$ )

